# Direct Observation of Reversible Electronic Energy Transfer Involving an Iridium Center

Sergey A. Denisov,[†,‡] Yanouk Cudré,[§] Peter Verwilst,[†] Gediminas Jonusauskas,[‡] Marta Marín-Suárez,[∥] Jorge Fernando Fernández-Sánchez,[∥] Etienne Baranoff,*,[§] and Nathan D. McClenaghan*,[†]

[†]Université Bordeaux/CNRS, ISM, 351 cours de la Libération, 33405 Talence Cedex, France
[‡]Université Bordeaux/CNRS, LOMA, 351 cours de la Libération, 33405 Talence Cedex, France
[§]School of Chemistry, University of Birmingham, Edgbaston B15 2TT, United Kingdom
[∥]Department of Analytical Chemistry, Faculty of Sciences, University of Granada, Avenida Fuentenueva s/n, 18071 Granada, Spain

Ⓢ *Supporting Information*

ABSTRACT: A cyclometalated iridium complex is reported where the core complex comprises naphthylpyridine as the main ligand and the ancillary 2,2′-bipyridine ligand is attached to a pyrene unit by a short alkyl bridge. To obtain the complex with satisfactory purity, it was necessary to modify the standard synthesis (direct reaction of the ancillary ligand with the chloro-bridged iridium dimer) to a method harnessing an intermediate tetramethylheptanolate-based complex, which was subjected to acid-promoted removal of the ancillary ligand and subsequent complexation. The photophysical behavior of the bichromophoric complex and a model complex without the pendant pyrene were studied using steady-state and time-resolved spectroscopies. Reversible electronic energy transfer (REET) is demonstrated, uniquely with an emissive cyclometalated iridium center and an adjacent organic chromophore. After excited-state equilibration is established (5 ns) as a result of REET, extremely long luminescence lifetimes of up to 225 μs result, compared to 8.3 μs for the model complex, without diminishing the emission quantum yield. As a result, remarkably high oxygen sensitivity is observed in both solution and polymeric matrices.

Reversible Electronic Energy Transfer

$\tau_{lum} = 225\ \mu s$
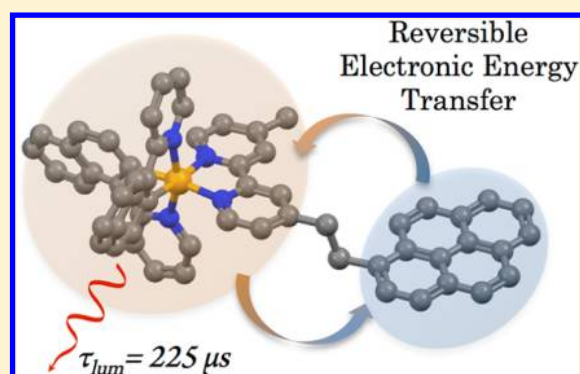
INTRODUCTION

Essential properties of transition-metal complexes that are intimately linked to the electronic and steric aspects of ligands in the primary coordination sphere include redox properties, light absorption, and emission. Additionally, in supermolecule complexes where spatially distinct chromophores are introduced, the latter may intervene in determining photophysical properties, for example, through electron or energy transfer.[1] Concerning emission, the quantum yield and luminescence lifetime are important characteristics, which ultimately define applicability in light-emitting and sensing architectures. We and others have previously applied an approach of harnessing *reversible* electronic energy transfer between energetically-matched chromophore pairs[2] exhibiting complementary kinetic behavior (see below and the Supporting Information, SI) in order to enhance the performance of several underperforming luminescent metal complexes based on ruthenium, osmium, copper, and rhenium as luminophores and photosensitizing agents.[3] Modification of the photophysical properties of cyclometalated iridium complexes is of particular interest because of their central role in multiple applications requiring highly efficient emission such as electroluminescence, sensing, and bioimaging.[4] Equally, this would add to the rather limited number of matched chromophore pairs.

In this context, here we report a straightforward structural modification of a cyclometalated iridium complex (see model complex **1**), involving the judicious integration of an auxiliary matched organic chromophore, in order to obtain a much longer-lived luminescent complex (**2**), while retaining a similar emission quantum yield. This modification could, in principle, broaden the scope of functions in multicomponent artificial photoactive arrays by changing excited-state properties, including the luminescence lifetime and oxygen sensitivity. A key to success was the introduction of a non-conjugated aliphatic spacer between the pyrene group and the adjacent 2,2′-bipyridine because direct attachment of the pyrene to the ancillary ligand results in quenching of the excited iridium center.[5]

The auxiliary organic chromophore was anticipated to play the desired role if the newly introduced triplet level was essentially isoenergetic with the emissive triplet metal-to-ligand charge-transfer (^{3}MLCT) state and exhibits slow inherent deexcitation. This would enable reversible intercomponent excited-state energy transfer, with the organic subunit acting as an energy reservoir, leading to a net luminescence lifetime

increase.[2] On the basis of luminescence data of **1**, vide infra, pyrene was selected as an appropriate candidate to play the desired role (triplet energy at 2.09 eV; τ_{phos} = 11000 μs);[6] see prototype **2** in Chart 1.

Chart 1. Structural Formulas of Iridium Complexes 1 and 2
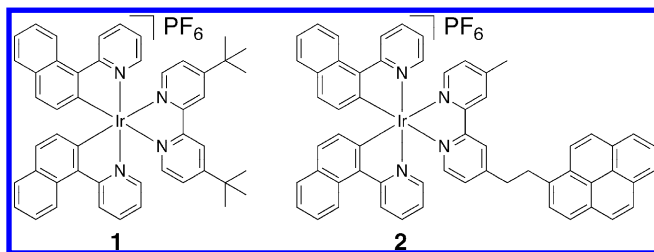
EXPERIMENTAL SECTION

General Procedures. All of the starting materials and solvents were commercially available and were used as received. Solvents and acids were received from Fisher except for diethyl ether (Sigma-Aldrich) and 2-ethoxyethanol (Acros Organics). Silica gel (60, 0.040−0.063 mm, 230−400 mesh) was received from Alfa Aesar, 2-bromopyridine (99%) from Aldrich, and tetrabutylammonium hydroxide (TBAOH·30H$_2$O) from Sigma-Aldrich; 1-naphthaleneboronic acid and tetrakis(triphenylphosphine)palladium(0) were received from Acros Organics and 2,2,6,6-tetramethyl-3,5-heptanedione, boron trifluoride diethyl etherate, and potassium hexafluorophosphate from Alfa Aesar; IrCl$_3$·xH$_2$O was received from Heraeus.

^{1}H NMR spectra were recorded using a Bruker AVIII 300 spectrometer, and ^{13}C NMR spectra were recorded using a Bruker AVIII 400 spectrometer. Chemical shifts (δ) were expressed in ppm and referenced to the residual CHCl$_3$ peak (7.26 ppm for ^{1}H and 77.16 ppm for ^{13}C). Coupling constants (J) are expressed in hertz (Hz). Mass spectrometry experiments were performed by means of electrospray ionization on a Synapt G2-S HDMS mass spectrometer (Waters Ltd., Manchester, U.K.) or a QStar Elite mass spectrometer (Applied Biosystems). Elemental analysis (C, H, and N) was performed on a Thermo Finnigan EA Flash 2000 analyzer at the CESAMO analytical center, University of Bordeaux, Talence, France.

Synthesis of Ir(npy)$_2$(tBubpy)(PF$_6$) (1). Compound **3** (100 mg, 0.079 mmol) was dissolved in a CH$_2$Cl$_2$/MeOH (9:1, v/v) mixture (20 mL) and degassed by bubbling argon. 4,4′-Di-*tert*-butyl-2,2′-bipyridine (85 mg, 0.316 mmol, 4 equiv) was added and the solution heated to reflux overnight under an argon atmosphere. The solvent was evaporated, and the remaining orange solid was dissolved in MeOH and precipitated with a saturated aqueous solution of KPF$_6$. The precipitate was filtered, washed with water and cold MeOH, and dried on the filter. The residue was washed with CH$_2$Cl$_2$. The solvent was reduced and added dropwise to Et$_2$O to precipitate **1** and remove the excess bipyridine. After filtration, **1** was obtained as an orange solid (114 mg, 0.112 mmol, 71%). ^{1}H NMR (300 MHz, CDCl$_3$): δ 8.55 (d, J = 8.5 Hz, 4H), 8.42 (s, 2H), 7.86 (t, J = 7.7 Hz, 2H), 7.74 (dd, J = 8.1 and 1.0 Hz, 4H), 7.68 (d, J = 5.8 Hz, 2H), 7.55 (ddd, J = 8.5, 6.9, and 1.3 Hz, 2H), 7.38 (t, J = 7.2 Hz, 2H), 7.31−7.23 (m, 4H), 7.17−7.08 (m, 2H), 6.26 (d, J = 8.3 Hz, 2H), 1.41 (s, 18H). ^{1}H NMR (300 MHz, CD$_3$CN): δ 8.64 (t, J = 8.7 Hz, 4H), 8.51 (d, J = 1.7 Hz, 2H), 7.95 (ddd, J = 8.6, 7.5, and 1.6 Hz, 2H), 7.78 (dd, J = 8.1 and 1.2 Hz, 2H), 7.75−7.69 (m, 4H), 7.58 (ddd, J = 8.5, 6.9, and 1.5 Hz, 2H), 7.45−7.36 (m, 4H), 7.33 (d, J = 8.3 Hz, 2H), 7.07 (ddd, J = 7.3, 5.8, and 1.3 Hz, 2H), 6.34 (d, J = 8.3 Hz, 2H), 1.39 (s, 18H). HRMS. Calcd: m/z 869.3189. Found: m/z 869.3206.

Synthesis of Ir(npy)$_2$(bpy-pyr)(PF$_6$) (2). Compound **5** (142 mg, 0.172 mmol) was dissolved in 20 mL of degassed CH$_2$Cl$_2$/MeOH (9:1, v/v). After further degassing, 4-methyl-4′-[2-(pyren-1-yl)ethyl]-2,2′-bipyridine (bpy-pyr; 103 mg, 0.258 mmol, 1.5 equiv) was added. The mixture was heated to reflux (40 °C) overnight under an argon atmosphere. The solvent was evaporated to dryness, and the crude

powder was dissolved in 20 mL of acetonitrile. A saturated aqueous solution of KPF$_6$ (100 mL) was added, and the mixture was stirred at room temperature for 1 h. The solvent was gently evaporated until a precipitate formed. The mixture was left in the a refrigerator for 2 h, and the precipitate was filtered, washed with water, and dried under vacuum. The powder was then dissolved in a minimum amount of CH$_2$Cl$_2$, precipitated in pure diethyl ether (to remove the remaining unreacted ligand), left in the freezer for 30 min, filtered, and washed with diethyl ether. The process was repeated. The complex was further purified by column chromatography on silica gel. The column was prepared with pure CH$_2$Cl$_2$, and the complex was adsorbed on the silica using pure CH$_2$Cl$_2$ as the eluent. The column was eluted first with CH$_2$Cl$_2$ to eliminate the fast-migrating impurities, and then the eluent was changed to CH$_2$Cl$_2$/acetonitrile (80:20, v/v) to collect an orange fraction. Anion exchange was performed again using acetonitrile and saturated KPF$_6$ in water, and **2** was obtained as an orange powder (0.160 g, 0.139 mmol, 81%). ^{1}H NMR (300 MHz, CDCl$_3$): δ 8.53 (dd, J = 10.3 and 6.7 Hz, 4H), 8.43 (d, J = 5.5 Hz, 2H), 8.20 (d, J = 9.3 Hz, 1H), 8.13 (t, J = 8.0 Hz, 2H), 8.05−7.90 (m, 5H), 7.88−7.77 (m, 3H), 7.72 (dd, J = 13.5 and 7.8 Hz, 2H), 7.65−7.43 (m, 6H), 7.37 (dt, J = 10.5 and 7.2 Hz, 2H), 7.24 (dd, J = 13.0 and 8.2 Hz, 2H), 7.10−6.99 (m, 2H), 6.99−6.91 (m, 1H), 6.86 (dd, J = 5.6 and 1.1 Hz, 1H), 6.25 (dd, J = 15.1 and 8.3 Hz, 2H), 3.86−3.65 (m, 2H), 3.37 (t, J = 7.5 Hz, 2H), 2.51 (s, 3H). HRMS. Calcd: m/z 999.3039. Found: m/z 999.3014. Anal. Calcd for C$_{59}$H$_{44}$F$_6$IrN$_4$OP (**2**·H$_2$O): C, 60.97; H, 3.82; N, 4.82. Found: C, 60.91; H, 3.72; N, 4.94.

Spectroscopy. Solutions for spectroscopic studies were degassed by multiple freeze−pump−thaw cycles, and the cell was blowtorch-sealed. Electronic absorption spectra were recorded on dilute solutions in 1 cm quartz cells using a Varian Cary-50 spectrophotometer. The picosecond transient absorption setup was built as follows. The frequency-tripled Nd:YAG amplified laser system (30 ps, 30 mJ at 1064 nm, 20 Hz, Ekspla model PL 2143) output was used to pump an optical parametric generator (Ekspla model PG 401), producing tunable excitation pulses in the range 410−2300 nm. The residual fundamental laser radiation was focused into a high-pressure xenon-filled breakdown cell, where a white-light pulse for sample probing was produced for nanosecond timescale measurements. For longer timescales (micro- and milliseconds), the white-light probe was obtained using an ensemble of light-emitting diodes (Roithner Lasertechnik, from 365 to 710 nm) working in flash mode, coupled with a multifurcated fiber-optic cable (eight cores, Avantes). All light signals were analyzed by a spectrograph (Princeton Instruments Acton model SP2300) coupled with a high-dynamic-range streak camera (Hamamatsu C7700). Accumulated sequences (sample emission, probe without and with excitation) of pulses were recorded and treated by *HPDTA* (Hamamatsu) software to produce two-dimensional maps (wavelength vs delay) of transient absorption intensity in the range 300−800 nm. The typical measurement error was better than 10^{-3} O.D. Emission spectra were recorded on the steak camera setup (uncorrected) and a Horiba Jobin Yvon Fluorolog 3 equipped with a Hamamatsu R928P PMT (corrected, Figure 2). Emission quantum yields (Φ) of the complexes were determined upon comparison with an optically dilute [Ru(bpy)$_3$]Cl$_2$ standard (Φ_r) in air-equilibrated water (Φ = 0.028)[6] according to the equation $\Phi = \Phi_r(I/I_r)(A_r/A)(\eta^2/\eta_r^2)$, where r refers to the reference sample, I is the integrated emission intensity, A is the absorbance at the excitation wavelength, and η is the refractive index of the solvent.

Samples were equally studied on the subpicosecond time scale: this experiment was based on a femtosecond 1 kHz Ti:sapphire system producing 30 fs, 0.8 mJ laser pulses centered at 800 nm (Femtopower Compact Pro) coupled with an optical parametric generator (Light Conversion Topas C), and frequency mixer was used to excite samples at the maximum of the steady-state absorption band. White-light continuum (360−1000 nm) pulses generated in a 2 mm D$_2$O cell were used as the probe. The variable delay time between excitation and probe pulses was obtained using a delay line with 0.66 fs resolution. The solutions were placed in a 2 mm circulating cell. White-light signal and reference spectra were recorded using a two-channel fiber spectrometer (Avantes Avaspec-2048-2). A home-written acquisition

Scheme 1. Synthesis of Dyes 1 and 2^a
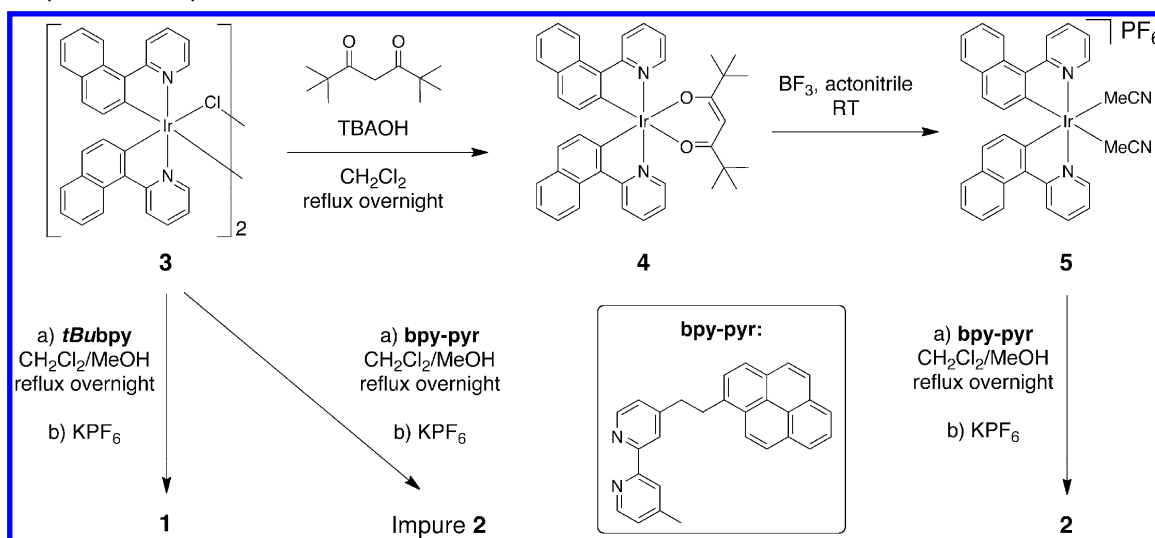
^{a}tBubpy = 4,4′-di-*tert*-butyl-2,2′-bipyridine; TBAOH = tetrabutylammonium hydroxide.

and experiment control program in *LabVIEW* made it possible to record transient spectra with an average error of less than 10^{-3} O.D. for all wavelengths. The temporal resolution of the setup was better than 50 fs. A temporal chirp of the probe pulse was corrected by a computer program with respect to a Lorentzian fit of a Kerr signal generated in a 0.2 mm glass plate used in place of the sample.

Oxygen Sensing. To obtain the sensing films, different mixtures were prepared (dye concentration of 1.5 mg·mL^{-1}) and shaken on a Vortex-Genie 2 (Scientific Industries, Bohemia, NY) equipped with a homemade holder. A nanostructure prepared by Ilford Imaging Switzerland following the procedure previously published[7−9] was also used as the support matrix. This nanostructure is called AP200/19, and it is based on a poly(ethylene terephthalate) thin plate coated by courting coating with aluminum oxide hydroxide, which provides a positively charged nanostructured film with a pore diameter of 19 nm and a total pore volume of 20 mL·m^{-2}.

Once all of the components were dissolved in chloroform, a Laurell model WS-400B-6NPP/LITE spin coater (North Wales, PA) was used to spin-coat the respective mixture on the supports. Both polystyrene (PS) and AP200/19 membranes were transparent and showed a thickness between 2 and 7 μm.

The luminescence measurements were obtained by means of a Varian Cary-Eclipse luminescence spectrometer equipped with a xenon flash lamp, Czerny−Turner monochromators, and a R-928 photomultiplier tube with manual or automatic voltage. For gas mixing, two mass-flow controllers (MFCs) of type EL-FLOW model F-201CV Bronkhorst High-Tech (Ruurlo, The Netherlands) were connected to copper and stainless steel tubing. These tubes connect the MFCs and a flow-through cell specially designed for the spectrometer. The O$_2$-gas station was controlled by a home-written *LabVIEW 8.2* program connected to a Flow Bus interface (Bronkhosrt) that pilots the Bronkhosrt MFCs via RS-232. A time trace curve was used to record I_0 and the intensity I at different oxygen partial pressures, which were calculated from the measured oxygen/nitrogen flows, assuming a constant environmental pressure of 1000 mbar.

■ RESULTS AND DISCUSSION

Synthesis and Design. Naphthlypyridine (npy)-based cyclometalated iridium complexes display ^{3}MLCT-based emission centered around 600 nm, which can be fine-tuned depending on the coligands present in the primary coordination sphere.[10,11] The corresponding energy of the emissive state closely approaches that of the triplet state of pyrene (vide

supra), making this combination of chromophores potentially suitable to introduce reversible interchromophore electronic energy transfer within the complex and dramatically modify observed luminescence properties, as demonstrated for complexes based on other metals.[2] To test this possibility, two molecular cyclometalated iridium complexes were prepared, namely the model complex (**1**) and the related bichromophoric complex (**2**) having an appended pyrene group (Chart 1). The synthetic strategy employed to obtain **1** and **2** is shown in Scheme 1. Following standard protocols, the reaction of 2-(naphthalen-1-yl)pyridine[10] with iridium(III) chloride hydrate gave the corresponding chloro-bridged dinuclear iridium complex, **3**, which precipitated from the reaction solvent mixture 2-ethoxyethanol/water. Owing to the low solubility of this chloro-bridged dimer in common deuterated solvents (chloroform, dichloromethane, acetonitrile, and dimethyl sulfoxide), satisfactory ^{1}H NMR characterization was not possible and **3** was initially used without further purification. Complex **1** was synthesized directly from the dimer according to standard methods. Reaction with an excess of tBubpy in a CH$_2$Cl$_2$/MeOH solvent mixture followed by anion exchange with PF$_6^-$ gave **1** as an orange solid, which was reasonably soluble in CDCl$_3$ and CD$_3$CN.

The same standard protocol was employed for the synthesis of complex **2**, using bpy-pyr[12] as the ancillary ligand. However, the resulting material was contaminated with an unidentified impurity, as seen in ^{1}H NMR spectra (Figure S7 in the SI). Purification attempts by column chromatography, on 20 × 20 cm thin-layer chromatography plates, by reprecipitation, and by recrystallization were all unsuccessful.

To obtain pure **2**, an alternative synthetic strategy was devised (Scheme 1). Reacting the dimer with 2,2,6,6-tetramethylheptane-3,5-dione in the presence of TBAOH gave a mononuclear intermediate complex, **4**,[13] which is highly soluble in common organic solvents. When previous synthetic methods were adapted,[14,15] the ancillary ligand was removed upon reaction with BF$_3$ in acetonitrile to give the bis(solvato) complex **5**. This bis(acetonitrile) complex was subsequently reacted with bpy-pyr in a dichloromethane/MeOH solvent mixture, yielding pure **2** after anion metathesis and purification by column chromatography on silica gel. The complex was

characterized by ^1H NMR and high-resolution mass spectrometry (HRMS), and the purity was assessed by elemental analysis. This synthetic strategy provides both an approach to purification of chloro-bridged iridium dimers, if a chloride source is present during acid degradation of the acetylacetonate-based complex,[14] and a method to obtain bis(solvato) complexes without the use of silver salts to remove chlorides from the dimer.
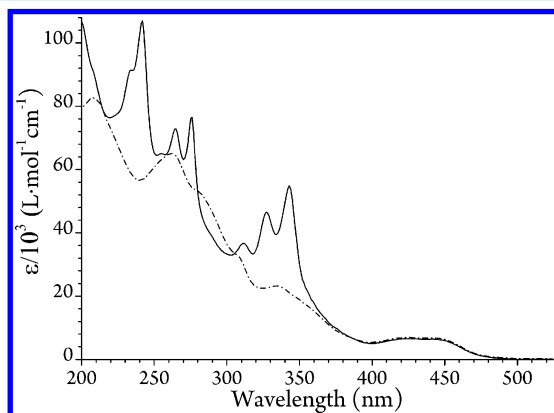
Electronic Absorption Spectroscopy. The photophysical properties of **1** and **2** are summarized in Table 1. Electronic

Table 1. Photophysical Properties of Iridium Complexes 1 and 2 in Acetonitrile at Room Temperature

complex	$\lambda_{em\ max}$ (nm)	Φ_{air}[a]	Φ_{degas}[b]	$\tau\ (\mu s)$[c]	K_{eq}[d]
1	590, 625	3.8×10^{-3}	10×10^{-2}	8.3 ± 0.3	
2	590, 625	5×10^{-4}	9.5×10^{-2}	225 ± 15	27.8 ± 2

[a]Luminescence quantum yield in an air-equilibrated CH_3CN solution compared to $[Ru(bpy)_3]^{2+}$ (bpy = 2,2′-bipyridine) in H_2O. [b]Luminescence quantum yield in a degassed CH_3CN solution compared to $[Ru(bpy)_3]^{2+}$. [c]MLCT luminescence lifetime in dilute degassed CH_3CN. [d]Excited-state equilibration constant (see the main text).

absorption spectra of **1** and **2** in acetonitrile at room temperature (Figure 1) are dominated by ligand-based

Figure 1. Electronic absorption spectra of **1** (dot-dashed line) and **2** (solid line) in acetonitrile.

absorption bands in the UV spectral region, and similar MLCT absorption bands are observed in the visible spectral region for both molecules. Additional pyrene absorption bands are observed for **2**, which retain their vibronic fine structure, implying only weak ground-state coupling between the two chromophores due to the integrated aliphatic spacer unit. As such, each chromophore is anticipated to retain its own specific properties in the ensemble.

Emission Spectroscopy. Photoluminescence spectra show MLCT-based red emission for acetonitrile solutions of both **1** and **2** ($\lambda_{em\ max}$ = 625 nm; Figure 2) with similar emission quantum yields in degassed acetonitrile (Φ_{degas} = 0.1). However, a higher oxygen sensitivity is observed in **2** compared with **1**. While the latter molecule shows a Φ_{degas}/Φ_{air} ratio of 26, a much higher value of 190 is obtained with **2**, which is consistent with a much longer excited-state lifetime; which
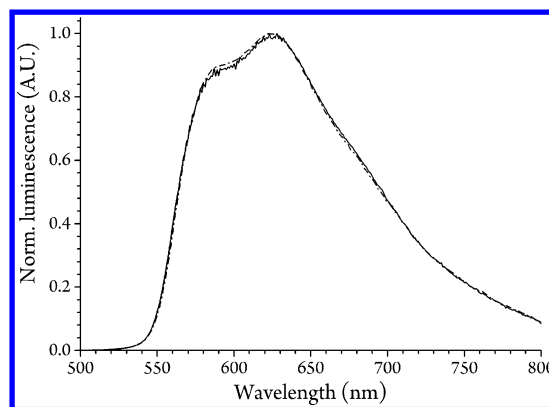
Figure 2. Photoluminescence spectra of **1** (dot-dashed line) and **2** (solid line) in degassed acetonitrile at room temperature (λ_{exc} = 413 nm).

would enhance diffusion-limited quenching by dissolved oxygen.

Time-Resolved Spectroscopy. Time-resolved spectroscopies in the subpicosecond to millisecond regimes give further information on the nature of the excited molecule and a clear insight into excited-state processes in the supermolecule. An emission lifetime of 8.3 μs was obtained for **1** in a degassed acetonitrile solution (Figure 3), while a luminescence lifetime
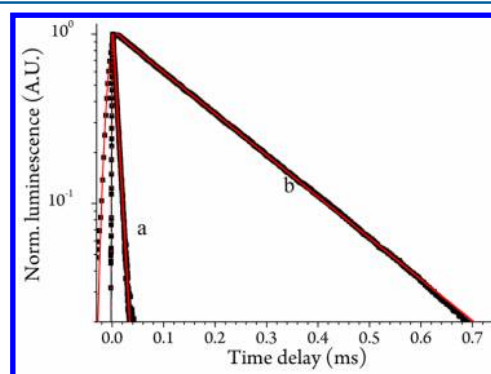
Figure 3. Luminescence decay in the 580−620 nm range of dilute **1** (a) and **2** (b) in degassed acetonitrile at room temperature (λ_{ex} = 465 nm).

that is over 25 times longer (215 ± 15 μs) was measured for a micromolar solution of **2**. Extrapolating to infinite dilution gave an apparent deexcitation rate of 4400 s^{-1}, or τ = 225 μs, much longer than that of the parent chromophore.

Complementary transient absorption spectroscopy elucidates the management of energy by the excited molecule prior to emission, and transient absorption signatures for both pyrene and iridium complexes have been described.[3,6,16,17] Excitation into the MLCT absorption band of **2** at 465 nm rapidly led to population of the pyrene triplet, denoted by a characteristic $T_n \leftarrow T_1$ absorption at 410 nm (see Figure 4). The kinetics of deexcitation of this absorption band exactly parallels those of the emission, clearly showing that while energy is principally located on this triplet (see the SI), it is quantitatively transferred to the metal center, where it is subsequently emitted. This observation implies the presence of quasi-isoenergetic excited states on the adjacent chromophores permitting rapid and reversible electronic energy transfer between them, leading to a dynamic excited-state equilibrium.
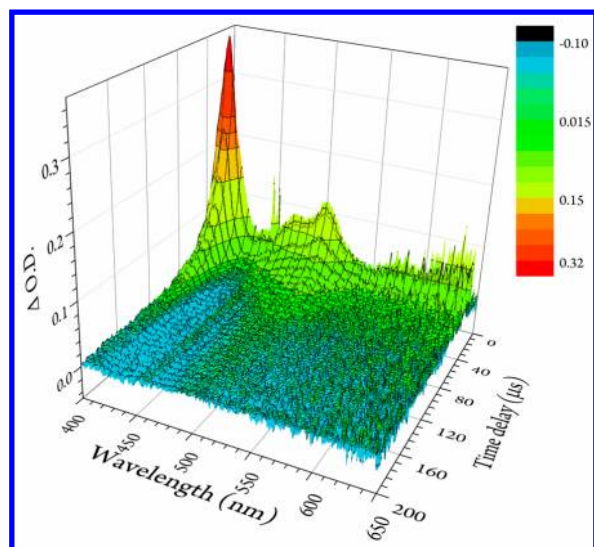
Figure 4. Transient absorption map of **2** showing deexcitation of the equilibrated bichromophoric molecule in acetonitrile at room temperature (λ_{ex} = 465 nm).

Low-temperature phosphorescence measurements were undertaken to elucidate the energies of the pertinent states and relative energy levels of **1** and **2**. At 77 K, MLCT emission ($\lambda_{em\ max}$ = 572 nm) could be observed from **1**, while emission of bichromophoric **2** was located further to the red ($\lambda_{em\ max}$ = 595 nm) and is ascribed to pyrene emission from this lower-lying state.[3,6] Assuming similar ^{3}MLCT levels in both complexes (at RT, they show similar emission spectra), only a small energy gap is expected between the pyrene triplet and the ^{3}MLCT state in **2**, which could enable reversible interchromophore electronic energy transfer at room temperature. Because such a small energy gap cannot be measured with sufficiently high precision in this fashion, the energy gap was determined using analysis of data from time-resolved spectroscopies (vide infra), which also gave unambiguous evidence for this unusual phenomenon.

The establishment of a dynamic excited-state equilibrium from an initial non-equilibrated excited state can be observed in real time by transient absorption spectroscopy, and a 5 ns rise time of the pyrene triplet absorption signature (see the SI) was measured. This value gives the rate of establishment of equilibrium (k = 2 × 10^8 s^{-1}) and is equal to the sum of the rate constants for forward (k_f) and backward (k_b) electronic energy-transfer processes.[2] The relative k_f and k_b values cannot be determined by direct observation based on transient absorption signatures because the iridium center ground-state bleaching signal overlaps with the transient MLCT absorption signal. Rather, along with the excited-state equilibrium constant (K_{eq}, which describes the distribution of energy between the constituent chromophores), k_f and k_b can be estimated using the inherent deexcitation properties of the constituent chromophores and the observed lifetime decay of **2** (τ_2 = 225 × 10^{-6} s), upon application of eqs 1 and 2, where τ_{MLCT} and τ_{pyr} correspond to the time constants for the decays of the excited iridium moiety and pyrene, respectively. α corresponds to the fraction of excited pyrene-like triplets, and (1 − α) corresponds to the fraction of excited MLCT-like triplets in the equilibrated population.

$$\frac{1}{\tau_2} = \alpha\frac{1}{\tau_{pyr}} + (1 - \alpha)\cdot\frac{1}{\tau_{MLCT}} \tag{1}$$

$$\frac{\alpha}{1 - \alpha} = K_{eq} = \frac{k_f}{k_b} \tag{2}$$

K_{eq} was thus estimated to be 27.8 ± 2, which means that the equilibrated population is predominantly (96.5%) in favor of the organic chromophore. Consequently, k_f and k_b were determined at 1.9 × 10^9 and 6.9 × 10^6 s^{-1}, respectively. Determination of K_{eq} allowed the energy gap between the triplet levels on the adjacent chromophores to be estimated at 680 cm^{-1} (assuming $\Delta E \approx -RT \ln K_{eq}$).

The ultrafast ^{1}MLCT-to-^{3}MLCT intersystem crossing (ISC) rate was estimated using femtosecond transient absorption spectroscopy upon excitation of the MLCT absorption band. On the basis of rapid changes in the spectrum at around 520 nm, the ISC rate was ca. 10 × 10^{12} s^{-1}. This high value corresponds to that previously determined (14 × 10^{12} s^{-1}) for related cyclometalated iridium complexes[17] and implies that, following excitation, ultrafast ISC precedes a slower inter-component energy transfer, which then leads to an excited-state equilibrium. The ensemble of rate constants for pertinent processes is shown in the Jablonski diagram in Figure 5.
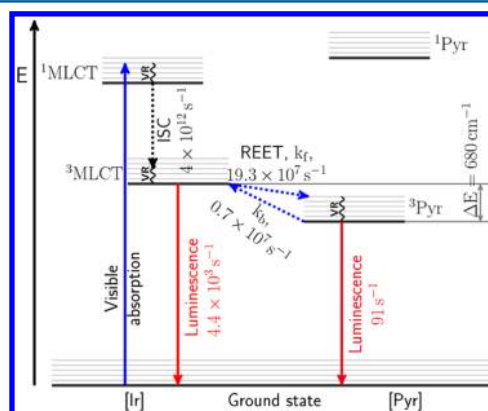
Figure 5. Jablonski diagram showing pertinent energy levels and kinetics of interchromophore energy transfer and luminescence of **2**. VR = vibrational relaxation, ISC = intersystem crossing, and REET = reversible electronic energy transfer. k_f and k_b correspond to the rates of forward and backward energy transfer, respectively.

Oxygen Sensing. Because a long excited-state lifetime is important for efficient oxygen detection using luminescent probes, the oxygen-sensing properties of dye **2** were evaluated in solid hosts. We followed our previously reported methodology measuring emission intensities, in both a polymeric PS membrane and a nanostructured metal oxide matrix (AP200/19).[18] A significantly better performance with AP200/19 compared to PS was observed because of improved oxygen permeability; between 0 and 10% O$_2$, the Stern−Volmer constants are 1103 and 294 bar^{-1} for AP200/19 and PS, respectively (see the SI). These results make **2** one of the most sensitive iridium-based dyes and is highly promising for lifetime-based sensing methods, which are currently being investigated.

■ CONCLUSION

In summary, time-resolved spectroscopies conclusively show for the first time that excited-state equilibration is reached in a

bichromophoric iridium complex after a few nanoseconds via reversible intercomponent electronic energy transfer and subsequent emission of **2** is delayed (τ = 225 μs), without compromising the emission quantum yield. As well as offering an extremely long excited-state lifetime, excellent initial results were obtained for low-concentration oxygen detection and are under further investigation. Additionally, a specific synthetic strategy was necessary to obtain **2** as a pure material. This strategy should prove useful in preparing pure chloro-bridged iridium dimers and bis(solvato) complexes without utilizing silver salts to remove chlorides.

■ ASSOCIATED CONTENT

Ⓢ Supporting Information

Additional synthetic procedures, NMR, transient absorption maps, kinetics, and oxygen sensing. This material is available free of charge via the Internet at http://pubs.acs.org.

■ AUTHOR INFORMATION

Corresponding Authors

*E-mail: e.baranoff@bham.ac.uk.
*E-mail: nathan.mcclenaghan@u-bordeaux.fr.

Notes

The authors declare no competing financial interest.

■ ACKNOWLEDGMENTS

■ REFERENCES

(1) Schanze, K. S.; Walters, K. A. Photoinduced Electron Transfer in Metal−Organic Dyads. In *Organic and Inorganic Photochemistry*; Ramamurthy, V., Schanze, K. S., Eds.; Marcel Dekker: New York, 1998; Vol. 2 of Molecular and Supramolecular Photochemistry, p 75.
(2) (a) Lavie-Cambot, A.; Lincheneau, C.; Cantuel, M.; Leydet, Y.; McClenaghan, N. D. *Chem. Soc. Rev.* **2010**, *39*, 506. (b) Wang, X.-Y.; Del Guerzo, A.; Schmehl, R. H. *J. Photochem. Photobiol. C* **2004**, *5*, 55. (c) Ford, W. E.; Rodgers, M. A. J. *J. Phys. Chem.* **1992**, *96*, 2917.
(3) (a) Ragazzon, G.; Verwilst, P.; Denisov, S. A.; Credi, A.; Jonusauskas, G.; McClenaghan, N. D. *Chem. Commun.* **2013**, *49*, 9110. (b) Ji, H.-F.; Shen, Y.; Hubner, J. P.; Carroll, B. F.; Schmehl, R. H.; Simon, J. A.; Schanze, K. S. *Appl. Spectrosc.* **2000**, *54*, 856. (c) Passalacqua, R.; Loiseau, F.; Campagna, S.; Fang, Y.-Q.; Hanan, G. S. *Angew. Chem., Int. Ed.* **2003**, *42*, 1608. (d) Tyson, D. S.; Castellano, F. N. *J. Phys. Chem. A* **1999**, *103*, 10955. (e) Hissler, M.; Harriman, A.; Khatyr, A.; Ziessel, R. *Chem.—Eur. J.* **1999**, *5*, 3366. (f) Simon, J. A.; Curry, S. L.; Schmehl, R. H.; Schatz, T. R.; Piotrowiak, P.; Jin, X.; Thummel, R. P. *J. Am. Chem. Soc.* **1997**, *119*, 11012. (g) Leydet, Y.; Bassani, D. M.; Jonusauskas, G.; McClenaghan, N. D. *J. Am. Chem. Soc.* **2007**, *129*, 8688. (h) Yarnell, J. E.; Deaton, J. C.; McCusker, C. E.; Castellano, F. N. *Inorg. Chem.* **2011**, *50*, 7820.
(4) (a) Costa, R. D.; Ortí, E.; Bolink, H. J.; Monti, F.; Accorsi, G.; Armaroli, N. *Angew. Chem.* **2012**, *51*, 8178. (b) You, Y.; Nam, W. *Chem. Soc. Rev.* **2012**, *41*, 7061. (c) Lowry, M. S.; Bernhard, S. *Chem.—Eur. J.* **2006**, *12*, 7970. (d) Lo, K. K.; Choi, A. W.; Law, W. H. *Dalton Trans.* **2012**, *41*, 6021. (e) Flamigni, L.; Barbieri, A.; Sabatini, C.; Ventura, B.; Barigelletti, F. *Top. Curr. Chem.* **2007**, *281*, 143.
(5) Constable, E. C.; Neuburger, M.; Rosel, P.; Schneider, G. E.; Zampese, J. A.; Housecroft, C. E.; Monti, F.; Armaroli, N.; Costa, R. D.; Ortí, E. *Inorg. Chem.* **2013**, *52*, 885.

(6) Montalti, M.; Credi, A.; Prodi, L.; Gandolfi, M. T. *Handbook of Photochemistry*, 3rd ed.; CRC/Taylor & Francis: London, 2006.
(7) Fernández-Sánchez, J. F.; Roth, T.; Cannas, R.; Nazeeruddin, M. K.; Spichiger, S.; Graetzel, M.; Spichiger-Keller, U. E. *Talanta* **2007**, *71*, 242.
(8) Marin-Suarez del Toro, M.; Fernandez-Sanchez, J. F.; Baranoff, E.; Nazeeruddin, M. K.; Graetzel, M.; Fernandez-Gutierrez, A. *Talanta* **2010**, *82*, 620.
(9) Medina-Castillo, A. L.; Fernandez-Sanchez, J. F.; Klein, C.; Nazeeruddin, M. K.; Segura-Carretero, A.; Fernandez-Gutierrez, A.; Graetzel, M.; Spichiger-Keller, U. E. *Analyst* **2007**, *132*, 929.
(10) Tian, N.; Thiessen, A.; Schiewek, R.; Schmitz, O. J.; Hertel, D.; Meerholz, K.; Holder, E. *J. Org. Chem.* **2009**, *74*, 2718.
(11) Zhen, H.; Luo, C.; Yang, W.; Song, W.; Du, B.; Jiang, J.; Jiang, C.; Zhang, Y.; Cao, Y. *Macromolecules* **2005**, *38*, 1693.
(12) McClenaghan, N. D.; Barigelletti, F.; Maubert, B.; Campagna, S. *Chem. Commun.* **2002**, 602.
(13) Jiang, J.; Jiang, C.; Wang, W.; Zhen, H.; Huang, F.; Cao, Y. *Macromolecules* **2005**, *38*, 4072.
(14) Baranoff, E.; Curchod, B. F. E.; Frey, J.; Scopelliti, R.; Kessler, F.; Tavernelli, I.; Rothlisberger, U.; Grätzel, M.; Nazeeruddin, M. K. *Inorg. Chem.* **2012**, *51*, 215.
(15) Zhou, Y.; Li, W.; Liu, Y.; Zhou, M. *ChemPlusChem* **2013**, *78*, 413.
(16) (a) Spaenig, F.; Olivier, J.-H.; Prusakova, V.; Retailleau, Z.; Castellano, F. N. *Inorg. Chem.* **2011**, *50*, 10859. (b) Ichimura, K.; Kobayashi, T.; King, K. A.; Watts, R. J. *J. Phys. Chem.* **1987**, *91*, 6104. (c) Li, Y.; Dandu, N.; Liu, R.; Hu, L.; Kilina, S.; Sun, W. *ACS Appl. Mater. Interfaces* **2013**, *5*, 6556. (d) Lafolet, F.; Welter, S.; Popovic, Z.; DeCola, L. *J. Mater. Chem.* **2005**, *15*, 2820.
(17) (a) Hedley, G. J.; Ruseckas, A.; Samuel, I. D. W. *J. Phys. Chem. A* **2009**, *113*, 2. (b) Tang, K. C.; Liu, K. L.; Chen, I.-C. *Chem. Phys. Lett.* **2004**, *386*, 437.
(18) Marín-Suárez, M.; Curchod, B. F. E.; Tavernelli, I.; Rothlisberger, U.; Scopelliti, R.; Jung, I.; Di Censo, D.; Grätzel, M.; Fernández-Sánchez, J. F.; Fernández-Gutiérrez, A.; Nazeeruddin, M. K.; Baranoff, E. *Chem. Mater.* **2012**, *24*, 2330.